Inorganic Chemistry

Article

pubs.acs.org/IC

Unusual Multi-Step Sequential Au^{III}/Au^{II} Processes of Gold(III) Quinoxalinoporphyrins in Acidic Non-Aqueous Media

Zhongping Ou,*[,†,‡] Weihua Zhu,[†,‡] Yuanyuan Fang,[‡] Paul J. Sintic,[§] Tony Khoury,[§] Maxwell J. Crossley,*[,§] and Karl M. Kadish*[,‡]

[†]School of Chemistry and Chemical Engineering, Jiangsu University, Zhenjiang 212013, China

[‡]Department of Chemistry, University of Houston, Houston, Texas 77204-5003, United States

[§]School of Chemistry, The University of Sydney, NSW 2006, Australia

ABSTRACT: The electrochemistry of gold(III) mono- and bis-quinoxalinoporphyrins was examined in CH_2Cl_2 or PhCN containing 0.1 M tetra-*n*-butylammonium perchlorate (TBAP) before and after the addition of trifluoroacetic acid to solution. The investigated porphyrins are represented as $Au(PQ)PF_6$ and $Au(QPQ)PF_6$, where P is the dianion of the 5,10,15,20-tetrakis(3,5-di-*tert*-butylphenyl)porphyrin and Q is a quinoxaline group fused to a *β*,*β*′-pyrrolic position of the porphyrin macrocycle; in $Au(QPQ)PF_6$ there is a linear arrangement where the quinoxalines are fused to pyrrolic positions that are opposite each other. The porphyrin without the fused quinoxaline groups, $Au(P)PF_6$, was also investigated under the same solution conditions. In the absence of acid, all three gold(III) porphyrins undergo a single reversible Au^{III}/Au^{II} process leading to the formation of a Au(II) porphyrin which can be further reduced at more negative potentials to give stepwise the Au(II) porphyrin *π*-anion radical and dianion, respectively. However, in the presence of acid, the initial Au^{III}/Au^{II} processes of $Au(PQ)PF_6$ and $Au(QPQ)PF_6$ are followed by an internal electron transfer and protonation to regenerate new Au(III) porphyrins assigned as $Au^{III}(PQH)^+$ and $Au^{III}(QPQH)^+$. Both protonated gold(III) quinoxalinoporphyrins then undergo a second Au^{III}/Au^{II} process at more negative potentials. The electrogenerated monoprotonated monoquinoxalinoporphyrin, $Au^{II}(PQH)$, is then further reduced to its *π*-anion radical and dianion forms, but this is not the case for the monoprotonated bis-quinoxalinoporphyrin, $Au^{II}(QPQH)$, which accepts a second proton and is rapidly converted to $Au^{III}(HQPQH)^+$ before undergoing a *third* Au^{III}/Au^{II} process to produce $Au^{II}(HQPQH)$ as a final product. Thus, $Au(P)PF_6$ undergoes one metal-centered reduction while $Au(PQ)PF_6$ and $Au(QPQ)PF_6$ exhibit two and three Au^{III}/Au^{II} processes, respectively. These unusual multistep sequential Au^{III}/Au^{II} processes were monitored by thin-layer spectroelectrochemistry and a reduction/oxidation mechanism for $Au(PQ)PF_6$ and $Au(QPQ)PF_6$ in acidic media is proposed.

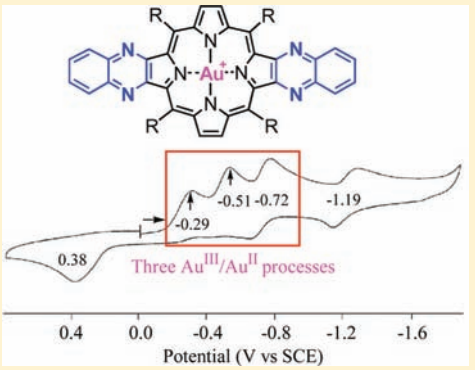

INTRODUCTION

The electron transfer reductions of quinoxalinoporphyrins can involve the central metal ion, the porphyrin macrocycle, or the fused quinoxaline group(s), all of which are redox active.[1−7] The sites of electron transfer, whether at the metal, at the macrocycle, or at the quinoxaline (Q) part of the molecule, are important factors to know and control since the electron transfer reactivity of these metalloporphyrins are directly related to their possible applications in photovoltaics[8,9] and molecular electronics.[10−23] Among the quinoxalinoporphyrins previously examined are the gold(III) derivatives which have been shown to undergo three or more one-electron reductions in nonaqueous media.[2−4,6,7] The first reduction is in almost all cases a metal-centered Au^{III}/Au^{II} process and leads to formation of an Au(II) porphyrin which can be further reduced at more negative potentials to give stepwise an Au(II) porphyrin *π*-anion radical and dianion under the given solution conditions. Further reductions beyond that of the Au(II) porphyrin dianion are also possible. These are located at the fused quinoxaline group and occur at potentials close to −2.0 V in the absence of electron withdrawing substituents on the macrocycle.[3,13]

The measured half-wave potentials for reduction of quinoxalinoporphyrins will depend upon the number of fused quinoxaline groups as well as upon the specific electron-donating or electron-withdrawing substituents on the macrocycle or Q group.[3,4,6,7,24] Shifts of redox potentials may also be seen upon changing the type of axial ligand on the metal center of the quinoxalinoporphyrin[21] or upon the binding of Sc^{3+} ions to the Q nitrogens of the quinoxalinoporphyrins in nonaqueous media, as was recently demonstrated for Au(III) mono- and bis-quinoxalinoporphyrins where the initial electroreduction was shifted from the Au(III) center to the quinoxaline part of the molecule.[5]

Protonation of the quinoxaline nitrogen atoms can also have a significant effect on the electrochemical behavior of quinoxalinoporphyrins as was demonstrated for derivatives

Received: September 6, 2011
Published: November 9, 2011

containing electrochemically inert Sn(IV), Cu(II), and Ni(II) central metal ions.[7] Because the fused quinoxaline group(s) can directly interact with the porphyrin π-ring system[5,19,20] one might reasonably predict the largest effect of protonation would be observed for ring-centered reductions and the smallest for metal-centered redox processes, but this has never been investigated in detail for quinoxalinoporphyrins with redox active central metal ions. It is also not known how protonation of the Q nitrogens would affect the site of electron transfer and reduction mechanism of quinoxalinoporphyrins with redox active central metal ions. Both points are addressed in the present study for two gold(III) quinoxalinoporphyrins, represented as Au(PQ)PF_6 and Au(QPQ)PF_6, where P is a dianion of the 5,10,15,20-tetrakis(3,5-di-*tert*-butylphenyl)-porphyrin and Q is the quinoxaline group fused on the β,β'-pyrrolic positions of the porphyrin macrocycle (Chart 1). As

Chart 1. Structures of the Investigated Gold(III) Porphyrins

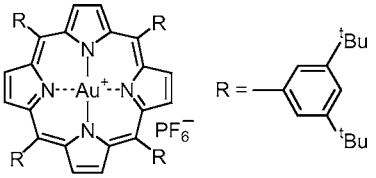

$Au^{III}(P)PF_6$ **1**

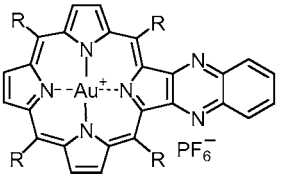

$Au^{III}(PQ)PF_6$ **2**

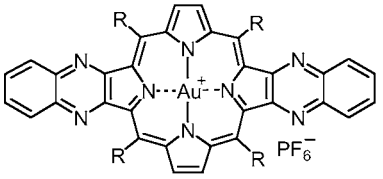

$Au^{III}(QPQ)PF_6$ **3**

will be demonstrated, the results are quite surprising in that Au(P)PF_6 undergoes one metal-centered reduction while Au(PQ)PF_6 and Au(QPQ)PF_6 exhibit two and three Au^{III}/Au^{II} processes, respectively. Combined data from electrochemistry and spectroelectrochemistry were utilized to elucidate the fate of the products after each electroreduction in dichloromethane or benzonitrile with and without added trifluoroacetic acid (TFA). The effects of the Q protonation on the site of electron transfer and spectra of the reduction products are discussed, and an overall reduction/oxidation mechanism for Au(PQ)PF_6 and Au(QPQ)PF_6 in acidic nonaqueous media is proposed.

RESULTS AND DISCUSSION

Electrochemistry of $Au^{III}(PQ)PF_6$. Au(P)PF_6 **1** exhibits two one-electron reductions in CH_2Cl_2 or PhCN containing 0.1 M tetra-*n*-butylammonium perchlorate (TBAP)[2,3] while three reversible electron additions are seen for Au(PQ)PF_6 **2** within the negative potential limit of the solvent.[3] The bis-quinoxalinoporphyrin, Au(QPQ)PF_6 **3**, also undergoes three one-electron reductions in these two solvents as shown in Figure 1 where cyclic voltammograms (CVs) of the three

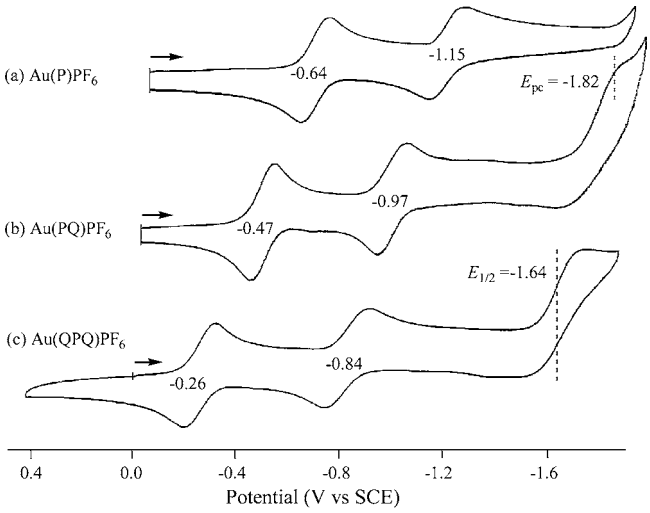

Figure 1. CVs of gold porphyrins in CH_2Cl_2 containing 0.1 M TBAP.

compounds are presented in CH_2Cl_2 containing 0.1 M TBAP. $E_{1/2}$ for the first one-electron reduction of the easiest to reduce QPQ complex (−0.26 V, Figure 1c) is positively shifted by 210 mV as compared to the PQ derivative ($E_{1/2}$ = −0.47 V, Figure 1b) and this $E_{1/2}$ value is positively shifted by 170 mV as compared to the same electrode reactions of the porphyrin in the absence of a fused quinoxaline group, that is, Au(P)PF_6 (−0.64 V, Figure 1a). A similar trend in $E_{1/2}$ values with increasing number of Q groups is seen for the second reduction of the three porphyrins and it has also been reported for a number of quinoxalinoporphyrins with redox inactive central metal ions.[3,7,25]

The first reversible one-electron reduction of all three porphyrins (Figure 1) is facile and metal-centered as characterized by Electron Spin Resonance (ESR) in the case of Au(P)PF_6 and Au(PQ)PF_6.[3] The approximately 800 mV separation between the second and the third reductions of $Au^{III}(PQ)^+$ and $Au^{III}(QPQ)^+$ is much larger than the average 450−500 mV separation reported for ring-centered reductions of mono- and bis-quinoxalinoporphyrins with redox inactive central metal ions,[4,7,25] but the redox processes in the case of the gold(III) derivatives are also assigned as occurring at the porphyrin π-ring system to give first an Au(II) porphyrin π-anion radical and then the corresponding dianion.

The addition of acid to quinoxalinoporphyrins in nonaqueous media can result in protonation of the quinoxaline nitrogens, either before or after electroreduction, and it was therefore necessary to examine UV−visible spectra of the starting compounds in acidic CH_2Cl_2 or PhCN solutions prior to carrying out the electrochemical measurements. The measured spectra of the unreduced compounds are shown in Figure 2a where the associated PF_6^- counterion is not included in the formula. $Au^{III}(P)^+$ in CH_2Cl_2 is characterized by a sharp Soret band at 415 nm and a single Q-band at 523 nm. The Soret bands of $Au^{III}(PQ)^+$ and $Au^{III}(QPQ)^+$ are also sharp and located at 435 and 450 nm, respectively, in neat CH_2Cl_2. Identical UV−visible spectra are obtained for each porphyrin in CH_2Cl_2 after addition of up to 100 equiv of trifluoroacetic acid (TFA) to solution, thus ruling out protonation of the neutral compounds under these experimental conditions.

dx.doi.org/10.1021/ic2019567 | Inorg. Chem. 2011, 50, 12802−12809

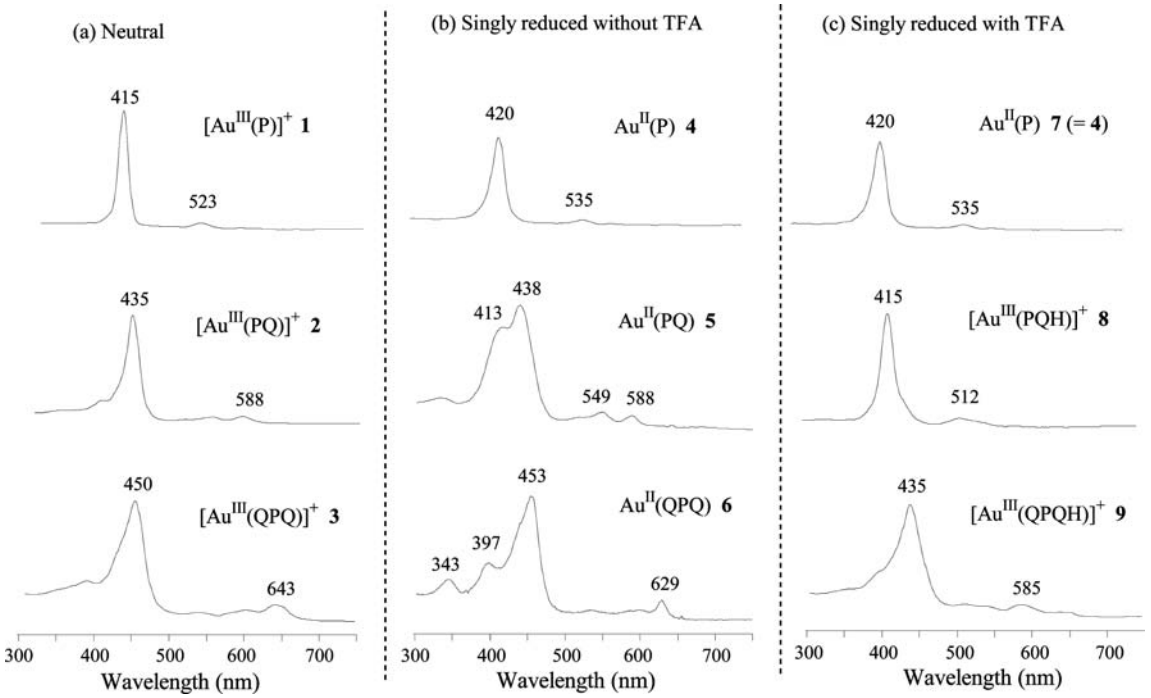

Figure 2. UV−visible spectra of gold(III) porphyrins in solutions of CH_2Cl_2 containing 0.1 M TBAP (a) before electroreduction, (b) after electroreduction in the same solution, and (c) after electroreduction in the same solution with 2−5 equiv of TFA.

The electrochemistry of $Au(P)^+$ in PhCN or CH_2Cl_2 (Figure 1a) is also invariant after adding TFA to solution and this contrasts with what is seen for $Au(PQ)^+$ and $Au(QPQ)^+$ where significant differences are observed in the CVs upon addition of 1−3 eq acid to solution. This is illustrated in Figure 3 for $Au(PQ)^+$ in PhCN containing 0.1 M TBAP and 1.5 equiv of TFA. Under these solution conditions the first metal-centered reduction at E_{pc} = −0.36 V is no longer reversible and the shape of the current−voltage curve is consistent with the occurrence of a fast chemical reaction following a reversible one-electron transfer.[26] The second, third, and fourth reductions which follow the initial metal-centered reduction of $Au^{III}(PQ)^+$ occur at $E_{1/2}$ = −0.60, −1.11, and −1.83 V. The $\Delta E_{1/2}$ between the second and third reductions in PhCN is 510 mV (Figure 3), and an identical $\Delta E_{1/2}$ is seen for the first two reductions of $Au^{III}(P)^+$ in CH_2Cl_2 (Figure 1a). $Au^{III}(PQ)^+$ also exhibits an irreversible oxidation in acidic media at E_{pa} = 0.34 V which is coupled to the first reduction (Figure 3). This oxidation is never seen for $Au^{III}(P)^+$, it is not seen for $Au^{III}(PQ)^+$ in acid solutions upon initial scans in a positive direction from 0.0 V (Figure 3, top), and it is also not observed prior to adding TFA to the solution.

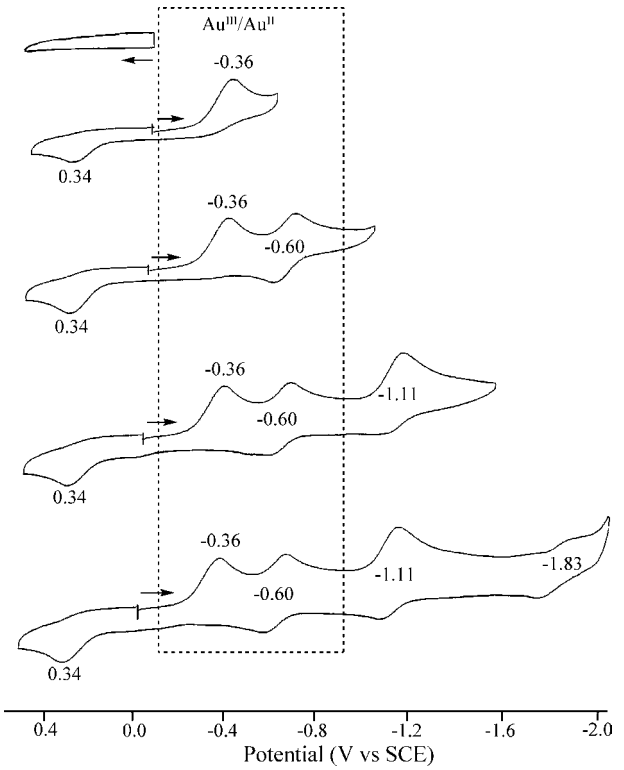

Figure 3. CVs of $Au(PQ)^+$ in PhCN with 1.5 equiv of TFA containing 0.1 M TBAP. Scan rate = 0.1 V/s.

We earlier reported that the first ring-centered one-electron reduction of $M^{II}(PQ)$ derivatives in PhCN containing added TFA is irreversible, resulting in formation of $M^{II}(PQH)$[7] which is then reduced to its π-anion radical and dianion forms at half-wave potentials which are 220−230 mV negative of $E_{1/2}$ values for reduction of the same quinoxalinoporphyrins in their unprotonated form. The overall shape of current−voltage curve in Figure 3 for reduction of $Au^{III}(PQ)PF_6$ in PhCN containing 1.5 equiv of TFA is similar to that reported for the reduction of Ni(II), Cu(II), and Sn(IV) quinoxalinoporphyrins in that an irreversible first reduction is followed by a second and third reversible one-electron addition at more negative potentials.[7] However, a major difference between the electrochemistry of $Au^{III}(PQ)^+$ and previously characterized $M^{II}(PQ)$ compounds is that the irreversible first reduction of the gold(III) quinoxalinoporphyrin at E_{pc} = −0.36 V is followed by *three* and not *two* one-electron transfers as occurs for the previously characterized protonated quinoxalinoporphyrins with redox inactive central metal ions.[7] The reason for the "extra" process after the first irreversible reduction of $Au^{III}(PQ)^+$ becomes

dx.doi.org/10.1021/ic2019567 | Inorg. Chem. 2011, 50, 12802–12809

quite clear upon analyzing UV−visible spectra obtained during electroreduction in a thin-layer cell which indicates that the final product of the first reduction is the protonated quinoxalinoporphyrin containing an Au(III) central metal ion, that is, $Au^{III}(PQH)^+$.

The relevant spectral data obtained during the three reductions of $Au^{III}(PQ)^+$ are shown in Figure 4. The product

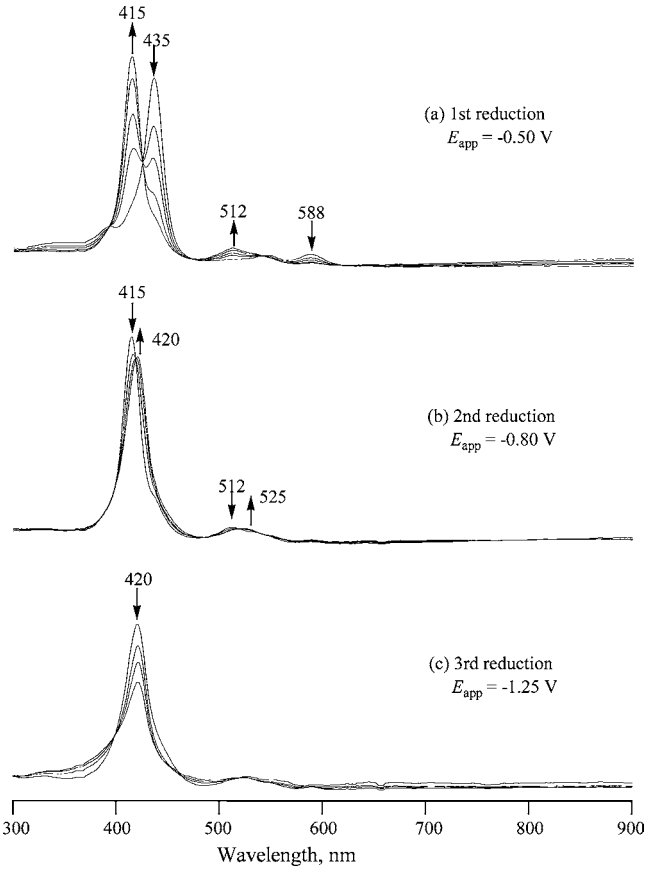

Figure 4. UV−vis spectral changes for $Au(PQ)^+$ in CH_2Cl_2 containing 0.1 M TBAP and ~2 equiv of TFA during reduction at (a) −0.50, (b) −0.80, and (c) −1.25 V.

of the one-electron reduction at a controlled potential of −0.50 V is characterized by a spectrum with a Soret band at 415 nm and single Q-band at 512 nm (Figure 4a). The UV−visible spectrum of unreduced $Au^{III}(P)^+$ also has a well-defined Soret band at 415 nm (**1** in Figure 2a) and both spectra are assigned as containing an Au(III) central metal ion. Further evidence in support of this oxidation state assignment for the singly reduced PQ compound is given by the spectroelectrochemical data in Figure 4b where the product of the second controlled potential reduction at −0.80 V has well-defined bands at 420 and 525 nm and is almost identical to the UV−visible spectrum of electrogenerated $Au^{II}(P)$ under the same solution conditions (see **7** in Figure 2b). The last two reductions of $Au^{III}(PQH)^+$ in Figure 3, at $E_{1/2}$ = −1.11 and −1.83 V, are assigned to occur at the porphyrin π-ring system, and the decreased intensity Soret band in the final spectrum after reduction at −1.25 V in the thin-layer cell (Figure 4c) suggests this assignment.

In summary, the overall reduction of $Au^{III}(PQ)^+$ in acidic nonaqueous media is proposed to occur as shown in Scheme 1 and involves *two* Au^{III}/Au^{II} processes being exhibited by $Au^{III}(PQ)^+$, one at E_{pc} = −0.36 V ($E_{1/2}$ = −0.39 V in the absence of acid) and the other at $E_{1/2}$ = −0.60 V. There is also a new irreversible oxidation peak at E_{pa} = 0.34 V in solutions of $Au^{III}(PQ)^+$ with TFA. This process involves an electrochemical "*EC*" mechanism, that is, an electrochemical conversion of $Au^{III}(PQH)^+$ to $Au^{III}(PQH)^{2+}$ (*E*) followed by loss of the proton on Q (*C*) and reformation of the original $Au^{III}(PQ)^+$ species at the electrode surface.

Electrochemistry of $Au^{III}(QPQ)PF_6$. The electrochemistry of $Au^{III}(QPQ)^+$ in CH_2Cl_2 containing 0.1 M TBAP is in many respects similar to what is described above for $Au^{III}(PQ)^+$ under the same solution conditions. In the absence of acid, three one-electron reductions are observed (see Figure 1c), the first of which is located at $E_{1/2}$ = −0.26 V and associated with an Au^{III}/Au^{II} process. The second reduction at $E_{1/2}$ = −0.84 V is assigned to formation of the Au(II) π-anion radical and the third at $E_{1/2}$ = −1.64 V to formation of the Au(II) porphyrin dianion. In the absence of acid the first two reductions are reversible on both the electrochemical and the spectroelectrochemical time scale, and UV−visible spectra obtained in a thin-layer cell during the first two controlled potential reductions at −0.40 and −1.00 V are given in Figure 5. The initial and final spectra of the singly reduced QPQ product in CH_2Cl_2 containing 0.1 M TBAP (without TFA) are also shown in Figure 2 where the compounds are numbered as **3** and **6**. As seen in these figures, the most intense Soret band shifts from 450 nm for $Au^{III}(QPQ)^+$ to 453 nm for $Au^{II}(QPQ)$ while the Q-band shifts from 643 to 629 nm upon conversion of Au(III) to Au(II). A small shift in λ_{max} values for the single Soret band peak with no change in shape of the spectrum is also seen upon conversion of $Au^{III}(P)^+$ to $Au^{II}(P)$ (see **1** and **4** in Figure 2), and this is consistent with the metal-centered electron transfer process.

Larger differences are seen in the overall spectral features of $Au^{II}(QPQ)$, $Au^{II}(P)$, and $Au^{II}(PQ)$ which differ in symmetry by virtue of the nature and placement of the fused Q groups. As seen in Figure 2b $Au^{II}(P)$ (**4**) exhibits a single Soret band at 420 nm, $Au^{II}(PQ)$ (**5**) exhibits a split Soret band at 413 and 438 nm, and $Au^{II}(QPQ)$ (**6**) shows three well-defined Soret bands located at 343, 397, and 453 nm.

Scheme 1. Proposed Reduction/Oxidation Mechanism of $Au(PQ)^+$ in Non-Aqueous Media Containing TFA[a]

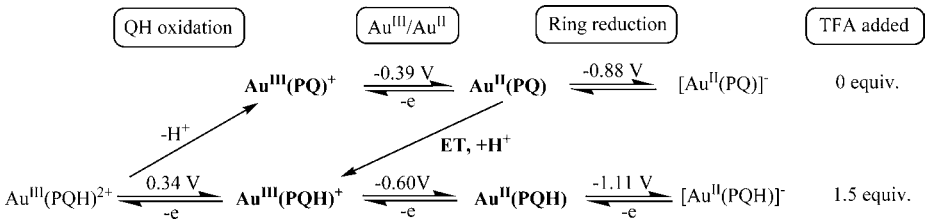

[a]The compounds in bold undergo the Au^{III}/Au^{II} process. The listed potentials were measured in PhCN, 0.1 M TBAP.

dx.doi.org/10.1021/ic2019567 | *Inorg. Chem.* 2011, 50, 12802−12809

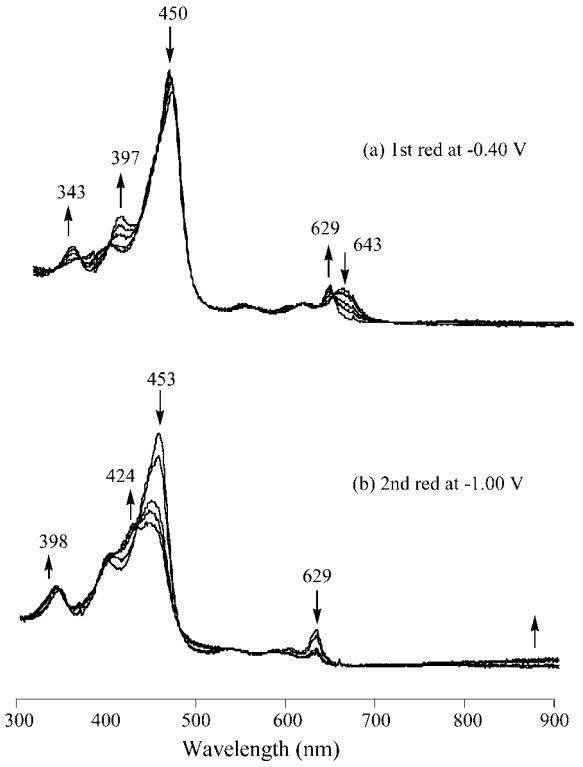

Figure 5. UV−vis spectral changes of $Au(QPQ)^+$ in CH_2Cl_2, 0.1 M TBAP during the first and second reductions under application of the indicated potentials.

Significant differences are also observed in the electrochemistry of $Au^{III}(QPQ)^+$ after the addition of TFA to solution. Two sequential metal-centered reductions (at E_{pc} = −0.31 and $E_{1/2}$ = −0.48 V) are seen in a CV of the compound when 1.0 equiv of TFA is added to a CH_2Cl_2 solution of $Au^{III}(QPQ)^+$ (Figure 6).

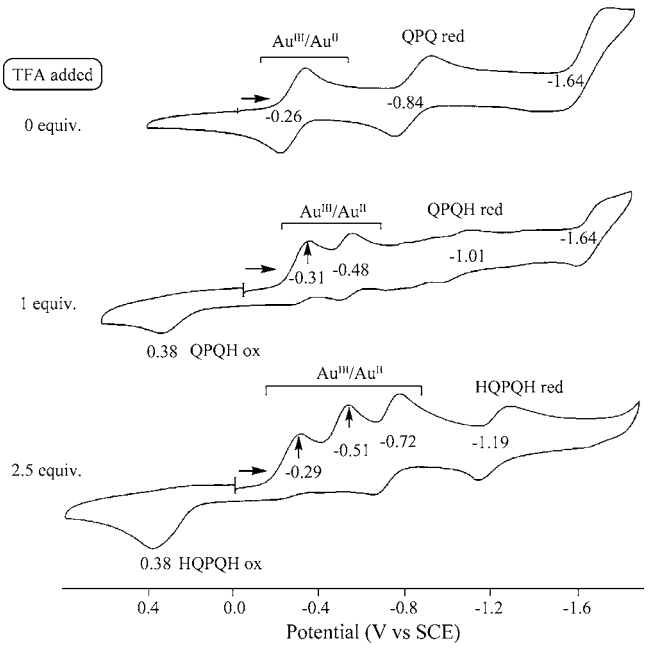

Figure 6. CVs of $Au(QPQ)^+$ in CH_2Cl_2 containing 0.1 M TBAP and added TFA. Scan rate = 0.1 V/s.

The CV of the bis-quinoxalinoporphyrin in the presence of 1.0 equiv of TFA is similar in shape and number of reduction processes to that for the monoquinoxalinoporphyrin, $Au^{III}(PQ)^+$ in the presence of 1.5 equiv of TFA (Figure 3). This is because only one of the two Q groups of $Au^{III}(QPQ)^+$ can be protonated upon the first one-electron reduction when the solution contains only one equiv of TFA. The first metal-centered reduction under these solution conditions is irreversible and, like in the case of $Au^{III}(PQ)^+$, this is due to an internal electron transfer and a quinoxaline group protonation, giving as a product of the homogeneous reaction the monoprotonated Au(III) bis-quinoxalinoporphyrin, $Au^{III}(QPQH)^+$. This monoprotonated Au(III) product of the first reduction can be reversibly reduced at E_{pc} = −0.48 V to give the monoprotonated Au(II) product, $Au^{II}(QPQH)$, or it can be reoxidized at E_{pa} = 0.38 V to give $Au^{III}(QPQH)^{2+}$ as seen by CVs in Figure 6. The oxidation follows an electrochemical *EC* mechanism and is assigned as a reversible electron abstraction followed by a rapid chemical reaction involving dissociation of the single proton on the Q group and reformation of the starting unprotonated porphyrin $Au^{III}(QPQ)^+$.

Three well-defined metal-centered reductions can be observed for $Au^{III}(QPQ)^+$ when 2.5 equiv of TFA are added to the CH_2Cl_2 solution. These sequential processes are located at E_{pc} = −0.29 and −0.51 and $E_{1/2}$ = −0.72 V (see Figure 7).

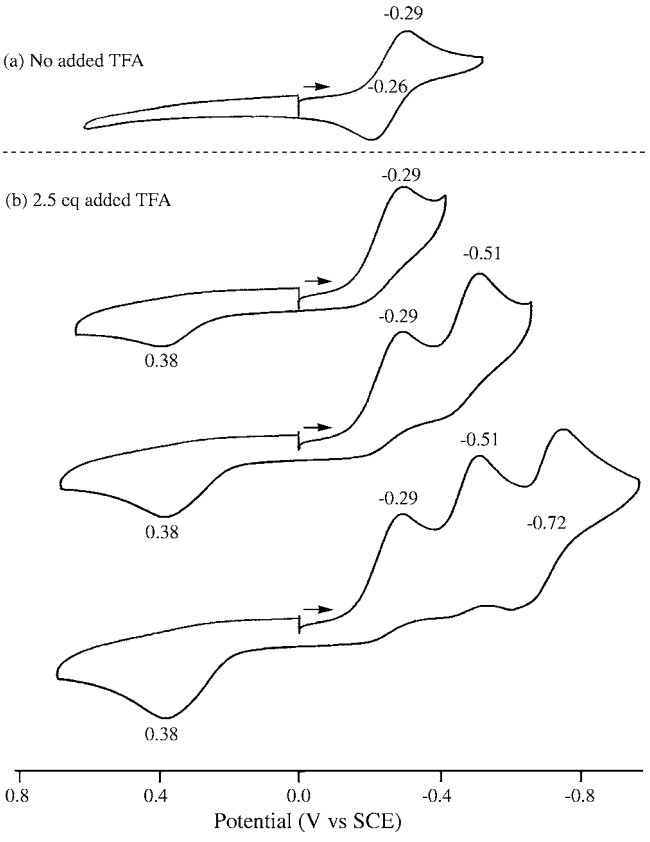

Figure 7. CVs showing Au(III) reductions of $Au(QPQ)^+$ in CH_2Cl_2 containing 0.1 M TBAP (a) before and (b) after 2.5 equiv of TFA have been added to solution.

All are assigned as involving a Au^{III}/Au^{II} process to give $Au^{III}(QPQH)^+$, $Au^{III}(HQPQH)^+$, and $Au^{II}(HQPQH)$ as sequential reduction products, with the proposed sequence of steps being given in Scheme 2.

The Au(III) mono- and bis-protonated bis-quinoxalinoporphyrins, $Au^{III}(QPQH)^+$ and $Au^{III}(HQPQH)^+$, generated after

dx.doi.org/10.1021/ic2019567 | *Inorg. Chem.* 2011, 50, 12802–12809

Scheme 2. Proposed Reduction/Oxidation Mechanism of $Au(QPQ)^+$ in Non-Aqueous Media Containing TFA[a]

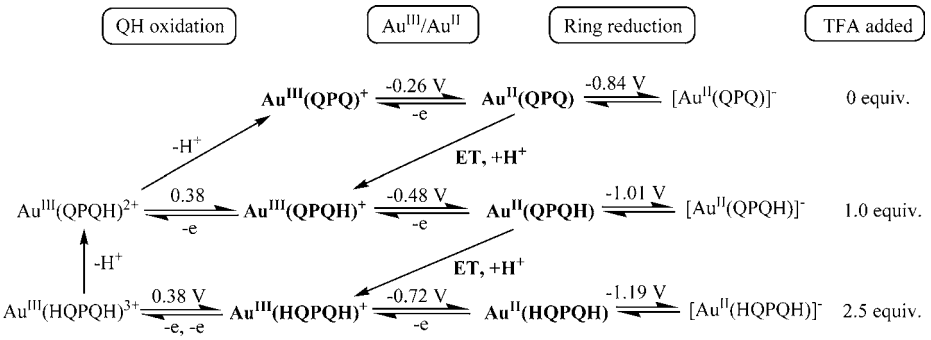

[a]The listed potentials were measured in CH_2Cl_2. The compounds in bold undergo the Au^{III}/Au^{II} process.

the reductions at E_{pc} = −0.29 and −0.51 V in CH_2Cl_2 with 1.0 equiv of added TFA can also be reoxidized at E_{pa} = 0.38 V to give $Au^{III}(QPQH)^{2+}$ and $Au^{III}(HQPQH)^{3+}$ prior to loss of one or two protons and reformation of the neutral compound, $Au^{III}(QPQ)^+$. Both reactions proceed via an *EC* mechanism which resembles that described above for $Au^{III}(PQ)^+$, the only difference being in the measured anodic peak potential of the oxidation peak which is 0.34 V in the case of $Au^{III}(PQH)^+$ and 0.38 V in the case of $Au^{III}(QPQH)^+$ and $Au^{III}(HQPQH)^+$.

As seen in Figure 7b, the peak current for the irreversible oxidation at E_{pa} = 0.38 V is approximately twice as high when the scan is reversed after the second metal-centered reduction at E_{pc} = −0.51 V. This result is consistent with one Q group being protonated after the first reduction and two Q groups being protonated after addition of the second. This interpretation is also consistent with the fact that the current for the irreversible oxidation of $Au(QPQ)^+$ in the presence of 2.5 equiv of TFA is also approximately double that when only 1.0 equiv of acid has been added to a solution of $Au^{III}(QPQ)^+$ (see Figure 6).

Thin-layer UV−visible spectral changes of $Au^{III}(QPQ)^+$ obtained during the first three controlled potential reductions in CH_2Cl_2 containing 0.1 M TBAP and ∼3 equiv of TFA as shown in Figure 8 differ from what is observed for the same compound in the absence of TFA (Figure 6). Under both solution conditions the initial bis-quinoxalinoporphyrin has a Soret band at 450 nm, a Q-band at 643 nm, and is unprotonated in its neutral form. When one electron is added during controlled potential reduction at −0.30 V in CH_2Cl_2 containing TFA (Figure 8a), the final product of the reaction has a single Soret band at 435 nm along with a Q-band at 585 nm. Both the reactant and the product are assigned as Au(III) porphyrins, that is, $Au^{III}(QPQ)^+$ and $Au^{III}(QPQH)^+$ (see also **3** and **9** in Figure 2).

Further reduction of $Au^{III}(QPQH)^+$ at −0.60 V in the acid containing solution gives a product with a single Soret band at 415 nm and a Q-band at 512 nm (Figure 8b). This spectrum is consistent with a species containing Au(III) porphyrin and is almost identical to the spectrum of $Au^{III}(P)^+$ which has bands at 415 and 523 nm (see **1** in Figure 2). The third reduction of $Au^{III}(QPQ)^+$ at a controlled potential of −0.80 V is also assigned to an Au^{III}/Au^{II} process but in this case no chemical reaction follows the electron transfer. The UV−visible spectrum for the stable product of the third reduction is shown in Figure 8c. It is characterized by a Soret band at 420 nm, a Q-band at 585 nm and is clearly diagnostic of an Au(II) porphyrin.

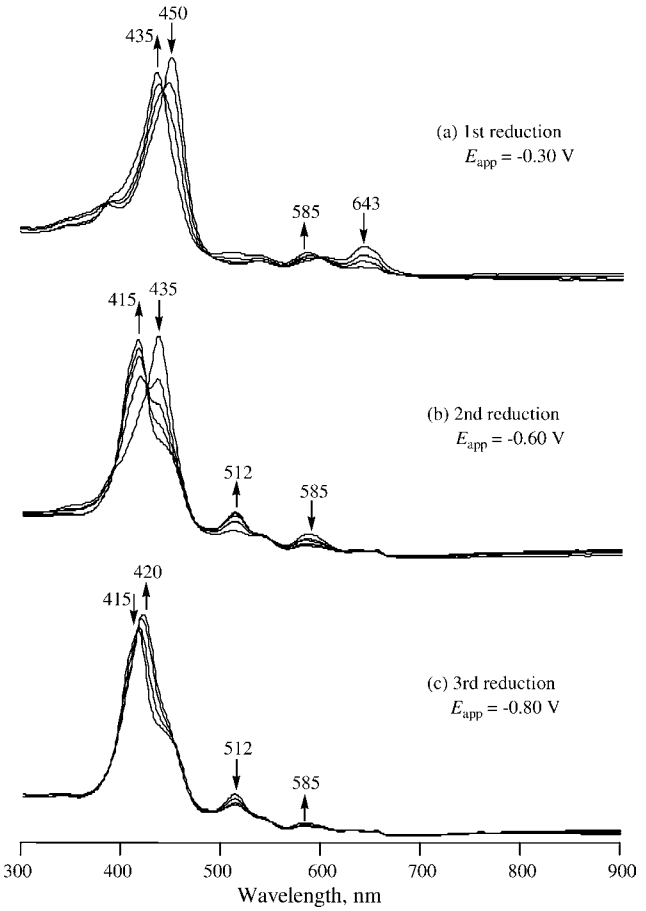

Figure 8. UV−vis spectral changes of $Au(QPQ)PF_6$ in CH_2Cl_2 containing 0.1 M TBAP and ∼3 equiv of TFA during reduction at (a) −0.30, (b) −0.60, and (c) −0.80 V.

Spectral Similarities between Protonated and Unprotonated Gold Porphyrins. Altogether six different Au(III) and three different Au(II) porphyrins were spectrally characterized in the presence of added acid. The data for these compounds are summarized in Tables 1 and 2, and examples of UV−visible spectra for the initial and singly reduced porphyrins are given in Figure 2. Three of Au(III) compounds have a Soret band at 415 nm, two have a Soret band at 435 nm and one has a Soret band at 450 nm. The identical Soret bands for each compound in the three groups of porphyrins suggest a quite similar extent of π-conjugation and charge distribution for each porphyrin in a given group, one comprising $Au^{III}(P)^+$,

dx.doi.org/10.1021/ic2019567 | Inorg. Chem. 2011, 50, 12802–12809

Table 1. UV-visible Spectral Data and Reduction Potentials (V vs SCE) of Au(III) Porphyrins in CH_2Cl_2 Containing 0.1 M TBAP and Added TFA

		UV−vis spectra		potential
Q number	compound	Soret band	Q-band	Au^{III}/Au^{II} process
none	$Au^{III}(P)^+$	415	523	−0.64
mono-Q	$Au^{III}(PQ)^+$	435	588	−0.36[a,b]
	$Au^{III}(PQH)^+$	415	512	−0.60[a]
bis-Q	$Au^{III}(QPQ)^+$	450	643	−0.29[b]
	$Au^{III}(QPQH)^+$	435	585	−0.48
	$Au^{III}(HQPQH)^+$	415	512	−0.72

[a]Measured in PhCN, 0.1 M TBAP. [b]Peak potential at a at scan rate of 0.10 V/s.

Table 2. UV-visible Spectral Data and Reduction Potentials (V vs SCE) of Au(II) Porphyrins in CH_2Cl_2 Containing 0.1 M TBAP and Added TFA

	UV−vis spectra		potential		
compound	Soret band	Q-band	ring reduction		ΔE (mV)[d]
$Au^{II}(P)$[a]	420	535	−1.09	1.81	720
$Au^{II}(PQH)$[a]	420	525	−1.11	−1.83	720
$Au^{II}(HQPQH)$	420	515	−1.19		
$Au^{II}(PQ)$[b]	413, 438	588	−0.97	−1.82[c]	850
$Au^{II}(QPQ)$[b]	343, 397, 453	629	−0.84	−1.64	800

[a]Potential measured in PhCN, 0.1 M TBAP. [b]Spectra and potential measured in solution without added TFA. [c]Peak potential at a scan rate of 0.10 V/s. [d]Potential difference between the two reductions.

$Au^{III}(PQH)^+$, and $Au^{III}(HQPQH)^+$ (415 nm), another $Au^{III}(PQ)^+$ and $Au^{III}(QPQH)^+$ (435 nm), and the third $Au^{III}(QPQ)^+$ (450 nm) (see Scheme 3).

A similar conjugated π-ring system is also suggested for the three Au(II) porphyrins, $Au^{II}(P)$, $Au^{II}(PQH)$, and $Au^{II}(HQPQH)$ in the presence of acid, all of which have a single intense Soret band at 420 nm (Scheme 3). These three Au(II) porphyrins also have similar reduction potentials for formation of the π-anion radical, that is, −1.09, −1.11, and −1.19 V (see Table 2).

The above results imply that conjugation between the porphyrin π-ring system and the β,β-fused Q group(s) of $Au^{III}(PQ)^+$ and $Au^{III}(QPQ)^+$ is interrupted upon protonation of the Q group(s), and thus similar spectra and similar reduction potentials are seen for $Au^{III}(P)^+$ and the two fully protonated Au(III) quinoxalinoporphyrins. The same can be said for the Au(II) porphyrins where the same spectral pattern is exhibited for $Au^{II}(HQPQH)$, $Au^{II}(PQH)$, and $Au^{III}(P)$, each of which is characterized by a Soret band at 420 nm. Again, the data suggests that conjugation between the Q group and the porphyrin macrocycle is interrupted upon protonation, and this is consistent with the electrochemical data described in the manuscript.

In summary, the electrochemical and spectroelectrochemical properties of $Au^{III}(P)^+$, $Au^{III}(PQ)^+$, and $Au^{III}(QPQ)^+$ were examined in CH_2Cl_2 containing 0.1 M TBAP. In the absence of TFA, each porphyrin undergoes one metal-centered reduction to form the corresponding Au(II) porphyrin, and this reaction is followed by two porphyrin ring-centered reductions leading to the formation of Au(II) π-anion radicals and dianions. Surprisingly, the two Au(III) quinoxalinoporphyrins in the presence of few equivalents of TFA will undergo unusual multistep sequential Au^{III}/Au^{II} processes because of an internal electron transfer and protonation of the fused Q group(s) on the porphyrin macrocycle. Thus, $Au(P)PF_6$ undergoes one metal-centered reduction while $Au(PQ)PF_6$ and $Au(QPQ)PF_6$ exhibit two and three Au^{III}/Au^{II} processes, respectively, in the presence of acid.

Finally, it is important to point out that the protonation which accompanies the reduction of $Au^{III}(PQ)^+$, $Au^{III}(QPQ)^+$, and $Au^{III}(QPQH)^+$ is reversible and the original compound can be regenerated by oxidation at a positive potential. These electrochemically initiated protonation and deprotonation steps change not only redox potentials of the compounds but also their UV−visible properties which may have possible application in building of ON-OFF switching devices.

EXPERIMENTAL SECTION

Instrumentation. Cyclic voltammetry was carried out at 298 K using an EG&G Princeton Applied Research (PAR) 173 potentiostat/galvanostat. A homemade three-electrode cell was used for cyclic voltammetric measurements and consisted of a platinum button or glassy carbon working electrode, a platinum counter electrode, and a homemade saturated calomel reference electrode (SCE). The SCE was separated from the bulk of the solution by a fritted glass bridge of low porosity which contained the solvent/supporting electrolyte mixture.

Thin-layer UV−visible spectroelectrochemical experiments were performed with a home-built thin-layer cell which has a light transparent platinum net working electrode. Potentials were applied and monitored with an EG&G PAR Model 173 potentiostat. Time-resolved UV−visible spectra were recorded with a Hewlett-Packard Model 8453 diode array spectrophotometer. High purity N_2 from Trigas was used to deoxygenate the solution and kept over the solution during each electrochemical and spectroelectrochemical experiment.

Chemicals. Benzonitrile (PhCN) was obtained from Aldrich Co. and distilled over P_2O_5 under vacuum prior to use. Dichloromethane (CH_2Cl_2) was obtained from Aldrich Co. and used as received for electrochemistry and spectroelectrochemistry experiments. TBAP was purchased from Sigma Chemical or Fluka Chemika Co., recrystallized from ethyl alcohol, and dried under vacuum at 40 °C for at least one week prior to use.

The syntheses of hexafluorophosphate[5,10,15,20-tetrakis(3,5-di-*tert*-butylphenyl)porphyrinato]aurate(III), $Au^{III}(P)PF_6$,[3] hexafluorophosphate{5,10,15,20-tetrakis(3,5-di-*tert*-butylphenyl)-quinoxalino-[2,3-*b*]porphyrinato}aurate(III), $Au^{III}(PQ)PF_6$,[13] and

Scheme 3. Soret Band Maximum of Investigated Compounds

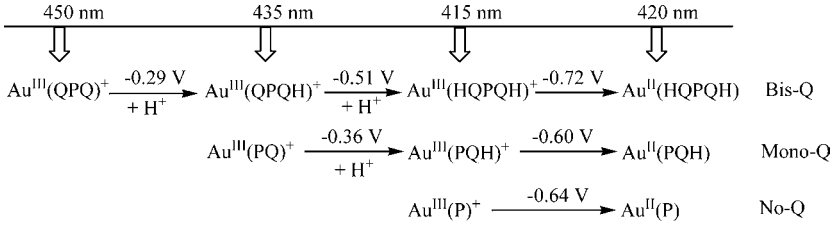

dx.doi.org/10.1021/ic2019567 | Inorg. Chem. 2011, 50, 12802–12809

hexafluorophosphate{5,10,15,20-tetrakis(3,5-di-*tert*-butylphenyl)-bisquinoxalino[2,3-*b*′:12,13-*b*″]porphyrinato}aurate(III),[5] $Au^{III}(QPQ)PF_6$ were published elsewhere.

AUTHOR INFORMATION

Corresponding Author

*E-mail: zpou2003@yahoo.com (Z.O.), m.crossley@chem.usyd.edu.au (M.J.C.), kkadish@uh.edu (K.M.K.).

ACKNOWLEDGMENTS

This work was supported by grants from the Robert A. Welch Foundation (K.M.K., Grant E-680) and the Natural Science Foundation of China (Grant 21071067). Support was also provided by a Discovery Research Grant (DP0208776) from the Australian Research Council to M.J.C.

REFERENCES

(1) Kadish, K. M.; Van Caemelbecke, E.; Rotal, G. In *The Porphyrin Handbook*; Kadish, K. M., Smith, K. M., Guilard, R., Eds.; Academic Press: New York, 2000; Vol. *8*, pp 1−114.

(2) Kadish, K. M.; E, W.; Ou, Z.; Shao, J.; Sintic, P. J.; Ohkubo, K.; Fukuzumi, S.; Crossley, M. J. *Chem. Commun.* **2002**, 356−357.

(3) Ou, Z.; Kadish, K. M.; E, W.; Shao, J.; Sintic, P. J.; Ohkubo, K.; Fukuzumi, S.; Crossley, M. J. *Inorg. Chem.* **2004**, *43*, 2078−2086.

(4) Zhu, W.; Sintic, M.; Ou, Z.; Sintic, P. J.; McDonald, J. A.; Brotherhood, P. R.; Crossley, M. J.; Kadish, K. M. *Inorg. Chem.* **2010**, *49*, 1027−1038.

(5) Ohkubo, K.; Garcia, R.; Sintic, P. J.; Khoury, T.; Crossley, M. J.; Kadish, K. M.; Fukuzumi, S. *Chem.—Eur. J.* **2009**, *15*, 10493−10503.

(6) Sintic, P. J.; E, W.; Ou, Z.; Shao, J.; McDonald, J. A.; Cai, Z.; Kadish, K. M.; Crossley, M. J.; Reimers, J. R. *Phys. Chem. Chem. Phys.* **2008**, *10*, 515−527.

(7) Ou, Z.; E, W.; Zhu, W.; Thordarson, P.; Sintic, P. J.; Crossley, M. J.; Kadish, K. M. *Inorg. Chem.* **2007**, *46*, 10840−10849.

(8) Kira, A.; Matsubara, Y.; Iijima, H.; Umeyama, T.; Matano, Y.; Ito, S.; Niemi, M.; Tkachenko, N. V.; Lemmetyinen, H.; Imahori, H. *J. Phys. Chem. C* **2010**, *114*, 11293−11304.

(9) Walter, M. G.; Rudine, A. B.; Wamser, C. C. *J. Porphyrins Phthalocyanines* **2010**, *14*, 759−792.

(10) Sharma, S.; Nath, M. *New J. Chem.* **2011**, *35*, 1630−1639.

(11) Eu, S.; Hayashi, S.; Umeyama, T.; Matano, Y.; Araki, Y.; Imahori, H. *J. Phys. Chem. C* **2008**, *112*, 4396−4405.

(12) Carroll, R. L.; Gorman, C. B. *Angew. Chem., Int. Ed.* **2002**, *41*, 4378−4400.

(13) Crossley, M. J.; Sintic, P. J.; Walton, R.; Reimers, J. R. *Org. Biomol. Chem.* **2003**, *1*, 2777−2787.

(14) Ohkubo, K.; Sintic, P. J.; Tkachenko, N. V.; Lemmetyinen, H.; E, W.; Ou, Z.; Shao, J.; Kadish, K. M.; Crossley, M. J.; Fukuzumi, S. *Chem. Phys.* **2006**, *326*, 3−14.

(15) Crossley, M. J.; Sintic, P. J.; Hutchison, J. A.; Ghiggino, K. P. *Org. Biomol. Chem.* **2005**, *3*, 852−865.

(16) Fukuzumi, S.; Hasobe, T.; Ohkubo, K.; Crossley, M. J.; Kamat, P. V.; Imahori, H. *J. Porphyrins Phthalocyanines* **2004**, *8*, 191−200.

(17) Fukuzumi, S.; Ohkubo, K.; E, W.; Ou, Z.; Shao, J.; Kadish, K. M.; Hutchison, J. A.; Ghiggino, K. P.; Sintic, P. J.; Crossley, M. J. *J. Am. Chem. Soc.* **2003**, *125*, 14984−14985.

(18) Yeow, E. K. L.; Sintic, P. J.; Cabral, N. M.; Reek, J. N. H.; Crossley, M. J.; Ghiggino, K. P. *Phys. Chem. Chem. Phys.* **2000**, *2*, 4281−4291.

(19) Crossley, M. J.; Prashar, J. K. *Tetrahedron Lett.* **1997**, *38*, 6751−6754.

(20) Khoury, T.; Crossley, M. J. *New J. Chem.* **2009**, *33*, 1076−1086.

(21) Hutchison, J. A.; Sintic, P. J.; Crossley, M. J.; Nagamura, T.; Ghiggino, K. P. *Phys. Chem. Chem. Phys.* **2009**, *11*, 3478−3489.

(22) Crossley, M. J.; Sheehan, C. S.; Khoury, T.; Reimers, J. R.; Sintic, P. J. *New J. Chem.* **2008**, *32*, 340−352.

(23) Fukuzumi, S.; Ohkubo, K.; Zhu, W.; Sintic, M.; Khoury, T.; Sintic, P. J.; E, W.; Ou, Z.; Crossley, M. J.; Kadish, K. M. *J. Am. Chem. Soc.* **2008**, *130*, 9451−9458.

(24) Kadish, K. M.; E, W.; Sintic, P. J.; Ou, Z.; Shao, J.; Ohkubo, K.; Fukuzumi, S.; Govenlock, L. J.; McDonald, J. A.; Try, A. C.; Cai, Z.; Reimers, J. R.; Crossley., M. J. *J. Phys. Chem. B* **2007**, *111*, 8762−8774.

(25) Ou, Z.; E, W.; Shao, J.; Burn, P. L.; Sheehan, C. S.; Walton, R.; Kadish, K. M.; Crossley, M. J. *J. Porphyrins Phthalocyanines* **2005**, *9*, 142−151.

(26) Bard, A. J.; Faulkner, L. R. *Electrochemical Methods, Fundamentals and Applications*, 2nd ed.; John Wiley & Son: New York, 2001.